Combustion and Flame 161 (2014) 1678–1686

Contents lists available at ScienceDirect

Combustion and Flame

journal homepage: www.elsevier.com/locate/combustflame

Plasma sheath behavior and ionic wind effect in electric field modified flames

Kunning Gabriel Xu

Mechanical & Aerospace Engineering Department, The University of Alabama in Huntsville, 301 Sparkman Dr., Huntsville, AL 35899, USA

ARTICLE INFO

Article history:
Received 3 July 2013
Received in revised form 17 October 2013
Accepted 6 December 2013
Available online 29 December 2013

Keywords:
Electric field modified flames
Plasma combustion
Ionic wind
Plasma sheath

ABSTRACT

Plasma sheath theory is applied to understand the plasma behavior in electric field modified flames. This paper presents a set of 1D plasma sheath equations with approximated analytical solutions to calculate the sheath thickness for given applied voltages and plasma properties. The results show that the anode sheath is ten of microns thick, less than 1 V, and largely independent of the applied voltage. The cathode sheath grows with the applied voltage to centimeters thick. The limited extent of the anode and cathode sheaths, which limits the reach of the electric field, in part explains the different flame behaviors reported in the literature. The ionic wind body force is also calculated based on ion energy losses due to collisions. The sheath analysis provides a possible explanation for reported flame behavior under a DC field modified such as saturation current and diode-like behavior.

1. Introduction

The ability of an electric field to modify flame behavior is well known. It was first reported by Chattock in 1899 [1]. Since then, a wide range of research has shown electric field induced changes in both premixed [2–9], and diffusion [10–12] flames. Some of the experimentally observed flame changes include increased flame speed [3,5,8,13,14], decreased lean blow-off equivalence ratio [5–7], decreased emissions and soot formation [10,15–17], and simulated gravity in diffusion flames [11]. Based on these results, the development of flame control methods using electric fields is promising. However, the basic interaction mechanism and physics is still unclear. In fact, the results tend to disagree on the magnitude and type of response.

Take for example, the laminar flame speed, the most widely reported measurement. Blair and Shen [4] and Bowser and Weinberg [18] showed very small changes <4% in flame speed using a flat flame with axial field. Comparatively, van den Boom et al. [3] showed an 8% increase in flame speed with a similar flat flame geometry, and Jaggers and Von Engel [14] showed a 100% increase in flame speed in a tube flame with transverse fields. Similar differences in field influenced flame speed changes have been reported for conical flames [5–8]. The reason for the differences is unknown, but may be related to experiment geometry or measurement technique. It has also been noticed that flame modifications only occur with a grounded burner such that ions are attracted upstream. The opposite configuration, a high voltage burner that repels ions, causes little to no change in the flame behavior. No physical explanation for this behavior has been found by the author.

There are also different theories for the cause of the observed flame behavior. An often referenced paper by Lawton and Weinberg [9] attributed the flame response to the ionic wind effect, a body force on ions due to the electric field. They analytically determined the maximum velocity, force, and static pressure a field can exert on the flame based on a maximum ion current density. Their results have been used by many researchers to support the ionic wind effect.

With all the research into this field, the exact mechanism and physics responsible for the flame modification is still unclear. The current literature discusses two causes for the flame response to an electric field: an electro-hydrodynamic effect (the ionic wind), or a change in flame kinetics from ion–electron recombination. Both of these theories have a commonality in the assumption of full electric field penetration into the bulk of the flame between the electrodes. Some early numerical simulations make this assumption as well by using a constant electric field [19]. This assumption neglects an important aspect of plasma, namely the plasma sheath and the non-uniform potential distribution and electric field. Some recent work has begun to discuss a non-uniform electric field. Goodings et al. modeled the floating potential distribution in a flame and discussed the presence of a sheath [20,21], Marcum and Ganguly measured the floating potential in a 15 kV field modified flame with a floating probe [13], van den Boom et al. briefly discusses the presence of the non-uniform field [3], and Belhi et al. numerically simulated the potential distribution in a diffusion flame under a 0.625 kV field [22]. These papers

E-mail address: gabe.xu@uah.edu

0010-2180/$ - see front matter © 2013 The Combustion Institute. Published by Elsevier Inc. All rights reserved.
http://dx.doi.org/10.1016/j.combustflame.2013.12.008

showed that the potential distribution is very non-uniform and is important to understand the electric field effect on the flame.

The goal of the present study is to investigate the impact and behavior of the plasma in electric field modified flames from a plasma physics perspective. An analytical model for the growth of the plasma sheath as a function of the potential is presented for the case of an ideal stoichiometric 1D premixed methane/air flat flame at 2210 K. The sheath thickness and the impacts on the electric field and ionic wind force are discussed. This work is a first step to examine the fundamental plasma behaviors and the interaction mechanisms in electric field modified flames.

2. Flame plasma sheath model

2.1. Flame plasma properties

Two primary properties of interest in plasma physics are plasma density and temperature. This can further be dividing into electron and ion specific densities and temperatures. For hydrocarbon flames, the ion number density has been both measured and computed to peak around 1×10^{10} cm^{-3} [23,24]. This is many orders of magnitude smaller than the neutral density, which at 1 atm and 2210 K is 3.3×10^{18} cm^{-3}. Nonetheless the flame plasma density is sufficiently high for noticeable effects under external fields. In hydrocarbon flames, the dominant positive species are H_3O^+ and CHO^+. The dominant negative species are electrons, followed far behind by O_2^- and CHO_2^-. These charged species are produced through chemical ionization in the reaction zone [9]. As with most other works in this field, we will consider H_3O^+ as the sole positive charge carrier and electrons as the sole negative charger carrier. The use of only H_3O^+ to account for ion species is due to its abundance downstream in the burnt gas as shown by Goodings et al. [23] and Prager et al. [24]. Most of the other positive ions disappear quickly outside the reaction region.

The average electron temperature of flame plasma can be taken equal to the flame temperature, assuming thermal equilibrium. For a stoichiometric ($\phi = 1$) methane–air flame, the adiabatic flame temperature is 2210 K, which equates to 0.19 eV [25]. The assumption of thermal equilibrium is valid as long as the collision frequency between electrons and neutrals is high. From kinetic theory, the collision frequency of a fast electron colliding with slow neutrals is $\nu_{en} = n_n \sigma_{en} \bar{\nu}_e$, where n_n is the neutral density, σ_{en} is the electron–neutral collision cross-section, $\overline{\nu_e} = \sqrt{8kT_e/\pi m_e}$ is the average electron thermal velocity, k is Boltzmann's constant, T_e is the electron temperature, and m_e is the electron mass. For the $\phi = 1$ flame considered here, taking the electron momentum transfer cross-section for N_2 ($\sigma_{en}(T_e = 0.19) = 7.9 \times 10^{-16}$ cm^2) [26] to represent the neutral flame species overall, the collision frequency is $\nu_{en} = 7.8 \times 10^{10}$ coll/s.

In the absence of an external field, the quasi-neutral assumption holds for flame plasmas, $n_i \approx n_e$. Along with the thermal equilibrium assumption, this means ions have the same energy as electrons and neutrals. The plasma density however is not uniform throughout space. As has been experimentally [27] and computationally [24] shown, the plasma density is a maximum in the reaction zone where ionization occurs and decreases both upstream and downstream. This drop in density can be attributed primarily to neutralization [9]. Charge loss can only occur through ion and electron collisions with surfaces, or each other. The charge particles have too low of an energy to cause collisional ionization of neutrals, and charge-exchange collisions with neutrals do not decrease the total charge. Neglecting surface neutralization, ion–electron recombination must be the dominate charge loss mechanism [9]. Recombination cross-section and rates for H_3O^+ have been measured by many researchers [28–33].

2.2. Plasma sheath

A short description of plasma sheaths and their behavior will be presented here for background. In short, the plasma sheath is a thin layer of plasma next to any surface immersed in plasma that transitions the potential from the plasma potential to the surface potential. The sheath arises due to the different thermal velocity and flux of ions and electrons. A flame is a weakly ionized plasma as mentioned. The electrons and ions are created within the reaction zone via chemi-ionization. Without an energizing field, the charged particles have low energies, 0.19 eV for a 2210 K flame, assuming thermal equilibrium. To a first order, the current flux per area of ions and electrons is,

$$\begin{aligned} J_i &= n_i e v_i \\ J_e &= n_e e v_e \end{aligned}, \tag{1}$$

where J is the current flux per area, e is the particle charge, n and v are the number density and thermal velocity, the i and e subscripts denote ions and electrons, respectively. The ratio of electron to ion flux, assuming quasi-neutral plasma, is simply the velocity ratio which is proportional to the square root of the mass ratio.

$$\frac{J_e}{J_i} = \frac{v_e}{v_i} = \sqrt{\frac{m_i}{m_e}}. \tag{2}$$

The ion mass is orders of magnitude larger than the electron mass, resulting in a disproportionate flux. In the example flame, the electron flux is 186 times larger than the H_3O^+ ($m_i = 3.16 \times 10^{-26}$ kg) flux. This difference can also been seen from their thermal velocities. For a temperature of 0.19 eV, H_3O^+ has a thermal velocity of 1570 m/s, while an electron has a thermal velocity of 300,000 m/s. This flux and velocity disparity creates the plasma sheath at a surface immerged in the plasma. Inside the plasma sheath, the quasi-neutral assumption is no longer valid and large electric fields and charge separation occurs.

Consider an unbiased or floating surface. The electron flux to the surface is much larger Thus at some initial time zero when the surface is first exposed to the plasma, the surface becomes negatively charged with respect to the plasma. This negative surface potential in turn repels electrons and attracts ions. The ion collection causes the surface potential to rises with respect to the initial negative potential at time zero. The surface potential thus rises and adjusts to retard the flux of electrons and increase the flux of ions to the surface until the fluxes balance, resulting in no net current. This adjustment occurs quickly, and can generally be considered instantaneous. The surface is now "floating" in the plasma at the floating potential, V_f which is below the plasma potential, V_p. The transition from the plasma potential to the floating potential occurs in a thin sheath layer next to the surface. Inside the sheath the local potential monotonically decreases from V_p to V_f as particles move toward the surface. The particle distribution inside the sheath is not uniform, typically resulting in increased ion density and decreased electron density closer to the surface. Thus the sheath is not quasi-neutral. This type of sheath is commonly called an ion sheath, or a negative sheath as the potential change is negative. Outside the sheath, the plasma is undisturbed and quasi-neutrality is maintained. Any flux of particle to the sheath edge is due to purely random thermal motion. The effect and presence of the surface does not impact the bulk plasma. In reality, there is not a sharply defined edge to the sheath. The definition is akin to a fluid boundary layer where the edge may be taken at 95% or 99% of the bulk potential.

Now consider the case of a biased electrode at a potential V. A positive electrode (anode) will collect a net electron current, and a negative electrode (cathode) will collect a net ion current. In both situations, the thermal electron flux is still much higher compared

to ions. Thus in most circumstances, the sheath is negative to reduce the electron flux to the electrodes. An electron or positive sheath (above plasma potential) that attracts electrons and repels ions is rare. This occurs only when a positive electrode draws more current than the random electron flux can provide. The maximum current density from random electron flux in a flame is approximately 960 A/m^2, much higher than any experimentally measured currents to date.

2.3. Sheath model

In plasma with an applied electric field, the effectiveness of the field is limited to within the electrode sheath. Thus the length or thickness of the sheath is important to understand the field effects. The sheath thickness depends on the plasma temperature, density, and the sheath potential drop, $V_s = V_p - V_f$ for a floating surface, or $V_s = V_p - V$ for a biased surface. For the case of a sheath potential much less than the electron temperature ($V_s \ll kT_e/e$), such as a floating surface, a Debye sheath develops. The sheath thickness is on the order of a few Debye lengths, $\lambda_D = (\varepsilon_o kT_e/n_e e^2)^{1/2}$ where ε_o is the permittivity of free space. The Debye sheath is largely independent of the applied voltage. A Debye sheath typically exists at anodes as will be shown later.

For the opposite case where the sheath potential is large ($V_s > kT_e/e$), the flux of charged particles and the sheath thickness becomes dictated by the potential. This generally occurs at the cathode as the difference between V_p and cathode potential is the largest in the system. At the cathode, the sheath potential is very negative and will fully repel electrons, creating a pure ion sheath. The solution for an ion sheath, which can be found in many texts on the subject [34–36], requires that ions enter the sheath with a minimum velocity. This is known as the Bohm sheath criterion, and it states that in order to have a monotonically decreasing potential from the bulk plasma to the wall, ions must enter the sheath edge with at least the Bohm velocity, $v_B = (kT_e/m_i)^{1/2}$, where m_i is the ion mass. The Bohm criterion creates a quasi-neutral region called the pre-sheath, wherein a small potential drop occurs between the bulk plasma and the sheath in order to minimally accelerate ions to the Bohm velocity. This Bohm pre-sheath potential is $V_B = kT_e/2e$. For a 2210 K flame, the pre-sheath potential is very small, less than 100 mV. However, this is sufficient to accelerate ions to the Bohm velocity of 980 m/s prior to the sheath. The pre-sheath exists for any ion collecting sheath. For a collisional pre-sheath, its length is approximately equal to the ion–neutral mean free path [37,38]. A diagram of the sheath and pre-sheath are shown in Fig. 1.

The thickness of an ion sheath can be determined by solving the conservation equations. The solution will differ depending on whether the sheath is collisionless or collisional. The collisionality of the plasma can be defined by a collision parameter, $\alpha = \lambda_D/\lambda_{MFP}$ where $\lambda_{MFP} = 1/n_n\sigma_{in}$ is the ion–neutral mean free path, and σ_{in} is the ion–neutral momentum transfer cross-section. A collisionless sheath is then defined as $\alpha \ll 1$, and a collisional sheath as $\alpha > 1$. Data on H_3O^+ momentum cross-sections with neutrals are not readily available, thus the N_2^+—N_2 cross-section will be used, $\sigma_{in}(0.19\ \text{eV}) = 1.39 \times 10^{-18}$ m^2.

To find solutions for the sheath thickness, we shall follow the model as given by Sheridan and Goree [39] for a collisional, unmagnetized plasma in contact with a biased planar surface. The solutions will be given here without proof. For more details please refer to the Appendix or Ref. [39]. Using non-dimensional variables $\eta = -eV_s/kT_e$, $\xi = x/\lambda_D$, and $u = v/v_B$, the sheath potential for a collisional sheath ($\alpha > 1$) is given by

$$\eta = \frac{3}{5}\left(\frac{3}{2}u_o\right)^{2/3}\alpha^{1/3}\xi^{5/3}. \tag{3}$$

Taking Eq. (3) at the wall ($\xi = d$, $\eta = \eta_w$), we obtain an expression for the collisional sheath thickness.

$$d = \left[\frac{500}{243}\frac{\eta_w^3}{\alpha u_o^2}\right]^{1/5}. \tag{4}$$

Similar expressions can be obtained for the opposite limit of a collisionless sheath:

$$\eta = \frac{3^{4/3}}{2^{5/3}}u_o^{2/3}\xi^{4/3}, \tag{5}$$

$$d = \frac{2^{5/4}}{3}\frac{\eta_w^{3/4}}{u_o^{1/2}}. \tag{6}$$

Flame plasma is highly collisional, thus the collisionless solutions are generally not very practical, but provides an illustration of the effect of collisionality. The sheath thickness based on Eqs. (4) and (6) for a range of collision parameters is shown in Fig. 2. A collisionless sheath is constant for small collision parameters and transitions to a collisional sheath around $\alpha = 1$. Combustion at atmospheric or higher pressures will generally be in the collisional regime. For example, an atmospheric pressure flame at 2210 K, assuming the plasma density and cross-section mentioned in Section 2, has a collision parameter of $\alpha = 150$ ($\lambda_D = 3.25 \times 10^{-5}$ m, $\lambda_{MFP} = 2.18 \times 10^{-7}$ m).

A plot of the sheath thickness for collisional and collisionless sheaths is shown in Fig. 3. The collisional sheath is thinner than a collisionless one at the same potential. This can be seen by

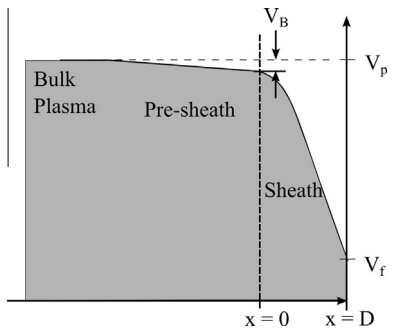

Fig. 1. Plasma sheath and pre-sheath potential near a boundary (not to scale). The sheath and pre-sheath are generally very thin. The sheath here is defined as from $x = 0$ to $x = D$.

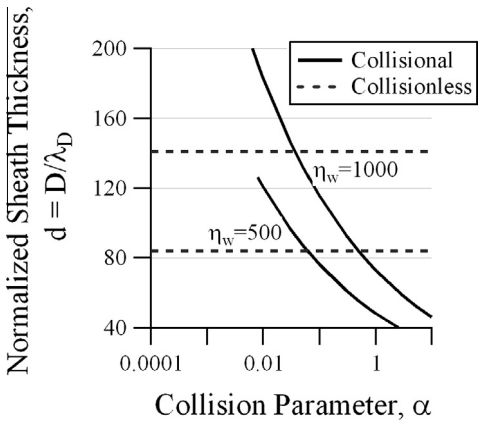

Fig. 2. Analytical solution of the sheath thickness for a range of collisional parameters. The limit approximations break down at the transition region around $\alpha = 1$. In the collisional regime, a higher collision parameters decrease the sheath thickness.

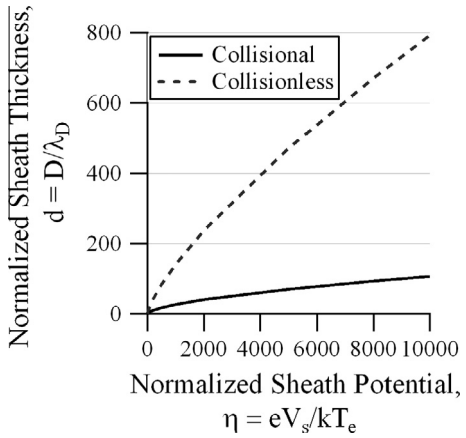

Fig. 3. Non-dimensionalized sheath thickness as a function of sheath potential for collisional and collisionless sheaths ($u_o = 1$, and $\alpha = 10.5$). The collisionless sheath is much thicker due to higher ion velocity, thus lower density, and consequently lower necessary electric field.

considering the ion motion and conservation equations. In a collisional sheath, the ion velocity is reduced by the neutral collisions, thus to maintain continuity the ion density must increase. An increase in density means increased electric field from Poisson's equation. For a given total sheath potential, the increased electric field means a thinner sheath. Lastly, Fig. 4 shows the collisional sheath thickness at three potentials for a range of plasma densities. As shown, the plasma density has a significant effect on the sheath through the collision parameter and Debye length. Physically this means for a given applied potential, the sheath must expand farther in a low density to accumulate sufficient particles for charge balance. Now that we have a method to calculate sheath thickness for collisional plasma, we can determine the effect of an electric field on flames.

An important detail to note is the sheath expansion area is not present. This 1D analysis only considers the sheath expansion away from a surface in a flat, top-hat profile. In reality the sheath will expand in 3D depending on the surface geometry. This may cause the total sheath area to increase with sheath thickness, and thus increase the particle flux and collected current. For example, a wire has a cylindrical sheath that grows in surface area as the sheath expands. A flat plate can have a top-hat sheath or a hemispherical sheath depending on the local plasma density and

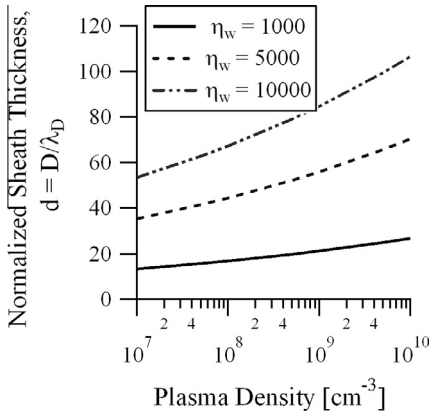

Fig. 4. Sheath thickness as a function of plasma density and potential. The sheath thickness is not only dependent on the applied potential, but also strongly affected by plasma density. As the flame plasma density tends to be spatially varying, the thickness of an actual flame sheath will differ from the 1D model.

boundaries. For simplicity, the analysis from here on will assume a uniform density.

3. Results and discussion

While a flame is only weakly ionized, charge conservation and quasi-neutrality still apply, and consequently plasma sheaths exist at the surface of electrodes. An analysis of the plasma sheath thickness and its effects will be performed for an ideal 1D flat flame as shown in Fig. 5. A stoichiometric premixed methane–air flame at atmospheric pressure is assumed. The top electrode acts as anode, and the burner head is the cathode. The cathode is grounded to provide a common reference potential. The electrodes have a potential difference V, separation distance h, and have a common area A. The power supply drives the anode positive relative to the cathode. This setup emulates many of the experiments reported in the literature [2,6,8,40]. The voltage, V, and separation distance reported in the literature has been from 50 to 5000 V and a few millimeters to centimeters, respectively.

In Fig. 5, the cathode sheath will be negative (electron repelling) since the cathode potential (0 V) is the lowest potential in the system. The anode sheath will also be negative, even though the anode is biased highly positive as previously discussed. For the purposes of this paper a voltage of 1 kV will be assumed.

The sheath potential and thereby thickness of the anode and cathode sheaths can be determined with a current balance. For a closed system, the current to the anode must be balance by the current to the cathode. A flame is not an ideal closed system, but will be assumed for simplicity. This net current is composed of the electron and ion flux to the anode sheath, $J_{a,e}$ and $J_{a,i}$, and the ion flux to the cathode sheath, $J_{c,i}$. The electron flux to the cathode will be assumed negligible as the cathode sheath is very negative, and thus repels all electrons. This will be shown mathematically later. The total current balance for the bulk plasma is thus

$$(J_{a,e} - J_{a,i})A_a = J_{c,i}A_c. \tag{7}$$

The electron and ion flux to the sheath can be calculated from Eq. (1). The plasma number density at the sheath edge can be calculated by substituting the Bohm potential into Boltzmann's equation for electrons,

$$n_s = n_o \exp\left(-\frac{eV}{kT_e}\right) = n_o \exp\left(-\frac{e}{kT_e}\frac{kT_e}{2e}\right) = 0.61 n_o, \tag{8}$$

where n_s is the plasma density at the sheath edge and n_o is the bulk plasma density away from the sheath. With quasi-neutrality assumed, the pre-sheath reduces the electron and ion density to 61% of the bulk density. An increased velocity decreases density from continuity. Both the anode and cathode sheath are electron repelling, or negative sheaths. The sheath thus accelerates ions toward the electrode, and it can be assumed all ions that enter the

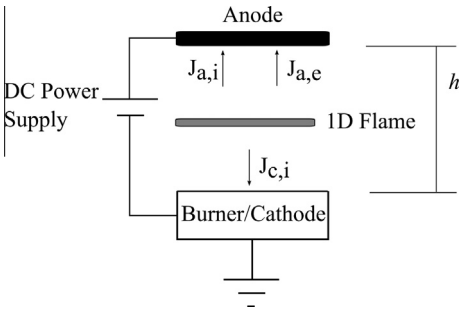

Fig. 5. 1D flat flame geometry used for analysis. The electrodes have separation distance d, area A, and ion and electrons currents densities J_e and J_i.

sheath edge are collected by the electrode. Electrons on the other hand are partially repelled by the negative sheath. Only electrons with sufficiently high energies reach the electrode. The electron density that reaches the anode through the sheath is thus further reduced according to Boltzmann's equation

$$n_{a,e} = n_{e,s} \exp\left(-\frac{eV_{a,s}}{kT_e}\right) = 0.61 n_o \exp\left(-\frac{eV_{a,s}}{kT_e}\right), \tag{9}$$

where $n_{a,e}$ is the electron density at the anode and $V_{a,s}$ is the anode sheath potential. The ion velocity is taken as the Bohm velocity at the sheath edge, and electron velocity is the thermal velocity. With Eq. (9) it is easy to show that the cathode sheath repels all electrons. The cathode is held at ground, which means the sheath must have a potential drop roughly equal to the applied bias. For an applied 1000 V with 0.19 eV electrons, the exponential term is effectively zero. Thus all electrons entering the cathode sheath are repelled. In fact, a potential drop of just 1 V is sufficient to repel 99.5% of the 0.19 eV electrons.

Putting Eq. (8) for ions and Eq. (9) for anode electrons into Eq. (7) gives

$$\left(en_{a,e}\sqrt{\frac{8kT_e}{\pi m_e}} - en_s\sqrt{\frac{kT_e}{m_i}}\right)A_a = \left(en_s\sqrt{\frac{kT_e}{m_i}}\right)A_c$$
$$0.61 en_o A_a \exp\left(-\frac{eV_{a,s}}{kT_e}\right)\sqrt{\frac{8kT_e}{\pi m_e}} = \left(0.61 en_o\sqrt{\frac{kT_e}{m_i}}\right)(A_c + A_a). \tag{10}$$

Solving for the anode sheath potential $V_{a,s}$ yields

$$V_{a,s} = \frac{kT_e}{e}\ln\left(\frac{A_c + A_a}{A_a}\sqrt{\frac{8\pi m_e}{m_i}}\right). \tag{11}$$

Eq. (11) relates the anode sheath potential drop necessary to maintain charge conservation to the plasma properties and electrode geometry. The equation also shows that the anode sheath is independent of the applied bias. For a given flame, the anode sheath potential and length will be approximately the same for all voltages. The electron temperature is the major driving factor presence in the anode sheath. Higher temperature electrons require more energy to repel.

For the case shown in Fig. 5 where $A_c = A_a$ and with H_3O^+ as the primary ion, the anode sheath potential is −0.56 V. The negative indicates a negative sheath, thus the anode must be below plasma potential. Since the anode potential is physically set by the power supply, the negative sheath actually pushes the plasma potential up by 0.56 V above the anode potential. With the anode sheath potential known, the cathode sheath potential can be determined by simply summing the anode and anode sheath potentials since the cathode is held at ground. Thus for a 1000 V anode, the cathode sheath potential drop is −1000.56 V.

Now that the sheath potentials are known, the reach of the electric field into flame can be calculated from the collisional sheath thickness given by Eq. (10). For these sheath potential values, the collisional anode sheath is 0.022 mm, and the cathode sheath is 1.8 mm. The pre-sheath length is much smaller at 2.2×10^{-4} mm, the ion–neutral mean free path. The additional increase in plasma potential caused by the anode sheath is negligible for these temperatures, thus the plasma potential and thereby cathode sheath potential can be taken as the applied voltage. Figure 6 shows the cathode sheath length as a function of the applied voltage for a cold (1600 K) and hot (2210 K) methane–air flame.

The results show that increasing the applied voltage on the electrodes grows the cathode sheath, but will have little to no effect on the anode sheath. The anode sheath will thus have little effect on the flame due to its small length. For the configuration considered here, as the burner or cathode sheath grows with increased voltage, a larger portion of the space between electrodes will experience an electric field. This means an increased number of ions will be accelerated and gain kinetic energy which can be transferred through collisions to the flow. This is especially the case if the sheath surface area grows, which is the common occurrence without physical boundaries.

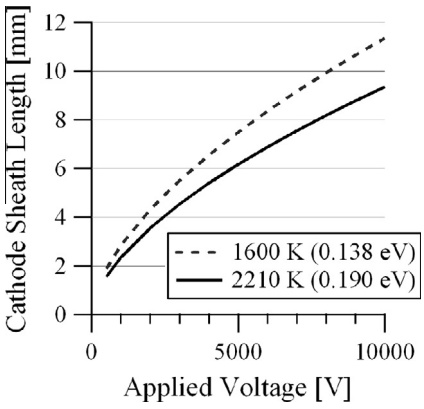

Fig. 6. The cathode sheath length increases nearly linearly with the applied voltage. A colder flame/plasma increases the sheath length. The anode sheath is independent of the applied voltage (for $n_i = 1 \times 10^{10}$ cm^{-3}).

A note should be made on the particle velocities used in the formulations. In Eq. (16), the ion current flux is taken at the sheath edge, after some minor pre-sheath ion acceleration. This allows the use of the Bohm velocity to simplify the solution, and is true for stationary plasmas. A flame plasma however is a flowing plasma with a mean velocity equal to the burnt gas velocity. The highly collisional nature of the flame means ions also have the same mean velocity. This flow velocity carries the ions toward the anode and away from the burner/cathode. At the downstream electrode, this means the pre-sheath does not need to provide as much acceleration to reach the Bohm velocity. At the burner, the ion flux is away from the burner, thus the pre-sheath must first decelerate the ions and then accelerate them upstream toward the burner to reach the Bohm velocity. The flowing plasma thus creates a slightly thicker burner pre-sheath and thinner downstream electrode pre-sheath, but the effect is small as the gas flow velocity is much smaller than the Bohm velocity. Likewise, replacing the anode ion flux velocity with the flow velocity in Eq. (10) causes minimal changes to the sheath potential. Thus for all practical purposes, the current formulation with the Bohm velocity is sufficiently accurate.

3.1. Ionic wind energy transfer to the flow

The body force known as the ionic wind is the primary suspect for alterations to a flame under an electric field. Lawton and Weinberg first proposed a maxima on the possible effects of an ionic wind based on the maximum ion current possible at air breakdown [9]. Their results gave a maximum static pressure of 40 N/m^2, and maximum force/volume of 8000 N/m^3, irrelevant of flame properties. Using the sheath analysis presented here, the energy deposited into the flow can be calculated based on ion–neutral collisions.

Ion and electrons gain kinetic energy from the electrostatic acceleration. Ions undergo momentum transfer collisions with neutrals, thereby injecting energy into the flow. Charge exchange collisions between ions and neutrals also occur, but shall be neglected for the momentum considerations. Electrons also undergo neutral collisions; however the large mass difference means any energy transfer likely goes into internal modes. Sheath theory says

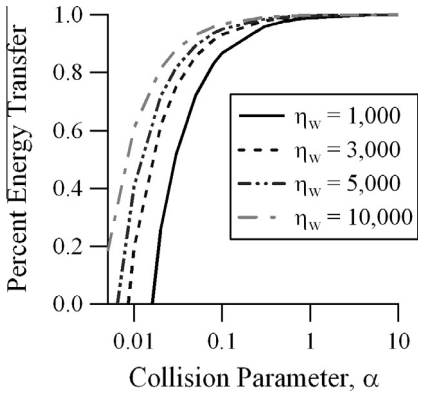

Fig. 7. Fraction of ion kinetic energy transferred to the flow for different collisional parameters and sheath potentials. Above $\alpha = 1$, 99% of the energy gained from the electric field is transfer into the flow. Thus for the majority of flames, all of the applied energy can be considered transferred to the flow.

large electric fields can only exist inside a sheath within a plasma. Thus we will assume any significant ion acceleration and momentum transfer only occurs within the sheath thickness, and primarily at the cathode for a grounded burner. A calculation of the energy transferred from the electric field to ions and then to neutrals can be obtained comparing the electrode impact energy of collisionless and collisional sheaths. Only the results are given below, a full derivation can be found in the Appendix.

The difference between the maximum impact energy from the collisionless case and the collisional case for a given sheath potential and collision parameter gives the total energy lost to the flow per ion.

$$\Delta\epsilon = \epsilon_{w,\alpha=0} - \epsilon_{w,\alpha>0} = \frac{1}{2}u_o^2 + \eta_w - \frac{1}{2}\left(\frac{5}{2}\frac{u_o\eta_w}{\alpha^{8/3}}\right)^{2/5}. \quad (12)$$

Eq. (12) can be converted to a force density and pressure with the ion density and distance over which the potential acts, i.e., the sheath thickness,

$$F = \frac{\Delta\epsilon k T_e n_i}{D}\ [\mathrm{N/m^3}], \quad (13)$$

$$p = \Delta\epsilon k T_e n_i\ [\mathrm{N/m^2}]. \quad (14)$$

Multiple factors affect the energy transfer from the field to the flow. Figure 7 shows the percent energy transferred to the flow ($\Delta\epsilon/\epsilon_{max}$) and shows that above $\alpha = 1$, 99% of energy goes into the flow, for any potential. As flames have collision parameters much greater than 1, this means that the flow will always collect all the power from the applied electric field. However, the electric power is at best a few watts, negligible compared to the thermal power of the flame. Thus the electric field does not contribute significant thermal energy to the flow. While collision parameters above one do not affect the fraction of energy transferred, it does greatly influence the force as shown in Fig. 8.

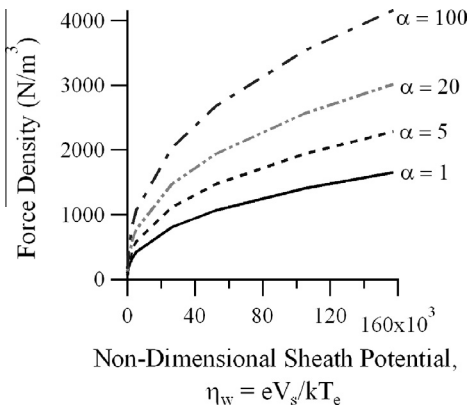

Fig. 8. The force density as a function of the sheath potential for different collisional parameters. While $\alpha > 1$ does not affect the percent energy transferred to the flow, it greatly affects the total force and thus pressure exerted by the ionic wind.

3.2. Discussion

The results of the sheath model can be used to examine reported data from literature. It is often noted that only a grounded burner causes noticeable flame changes, that a positive burner has no effect on the flame behavior. With sheath analysis, we can postulate an explanation for this behavior. When biased positively, the burner forms a micron-scale anode sheath. The anode sheath as shown is less than 1 V, and generally independent of the applied voltage. In most flames, the reaction zone sits ~1 mm above the burner, thus the anode sheath will not extend into the ion production region. Depending on electrode spacing, the thicker cathode sheath from the top electrode may not extend into the reaction zone either. This means only a fraction of the ions in the burnt product are accelerated by the electric field. The ion acceleration occurs downstream of and away from the flame front. Thus the ionic wind force caused by ion flow will not affect the actual flame. However, if the cathode sheath grew sufficiently large to extend into the flame front, effects such as lengthening of the flame should be possible.

Another behavior of the flame is a diode-like current response when the polarity is flipped. With a grounded burner, higher voltage produces higher current. A positive burner however produces nearly constant small current over a large range of voltages [13,21]. A possible explanation for this behavior can be seen from the sheath growth and flowing plasma. In the standard case of a grounded burner, the burner sheath and pre-sheath must overcome the mean flow velocity. A decrease in velocity results in an increase in density. Thus as the sheath grows, the amount of retreating ions collected is increased, which results in higher current. So increased ion current with voltage it is not merely an effect of higher ion acceleration, but an effect of sheath area coverage. In the opposite case with a positive burner, the sheath growth occurs from the top electrode down towards the incoming ions. As the ions are naturally convecting toward the sheath, the ion flux is dictated by the flow speed as previously mentioned. The burnt gas flow speed is relatively constant, thus an increased sheath thickness without an increase in area does not result in increased ion flux. Thus the positive burner case will reach current saturation quickly as seen in experiments [13,21].

The sheath also suggests a physical condition for the saturation current sometimes seen in flames. Current saturation occurs when increases in voltage does not result in a corresponding increase in ion current. This indicates that all ions present are being collected, or the collection equals the production. Considering the growing sheath and thus growing coverage of the flame/plasma volume, two likely conditions for saturation current is when the sheath fully covers the flame reaction zone, or the cathode and anode sheath meet. When the sheath, likely a cathode sheath due to its growth, covers the reaction zone, all ions produced there are immediately attracted to the burner. It may be possible for some ions with sufficient energy to escape, and chemi-ionization may also occur downstream of the reaction zone. At the second condition when both sheaths meet, the entire volume between the electrodes is under the influence of the electric field and all charged particles are collected. Further increases in voltage, prior

to breakdown, will not increase the total number of charged particles, only the amount of energy they have.

Finally, we can examine possible maximums of the ionic wind force from the sheath model. Lawton and Weinberg proposed maxima based on the minimum electric field required for breakdown in air, 30 kV/cm, and a given spacing of 0.5 cm between the flame and burner. From Eqs. (13) and (14), it is apparent that the pressure and force density from the sheath model cannot have a constant maximum for all possible flames. The three dimensional variables of T_e, n_i, and D will vary depending on flame geometry and properties. This makes sense since at initial breakdown, ionization of air molecules is very small. Only the high energy tail of the ion and electron energy distribution has just enough energy to cause collisional ionization of neutrals. This will limit the amount of secondary ions created via breakdown. As the electric field further increases, more secondary ions will be formed as more particles gain sufficient energy for ionization. At initial breakdown where Lawton and Weinberg take their maxima, the ion density should not be significantly higher than that produced by the flame. Thus the maximum current density should depend on the flame properties.

Using values for density and temperature previously assumed, and an electric field of 30 kV/cm with 0.5 cm separation, the ionic wind pressure and force density from this model are 24 N/m^2 and 4800 N/m^3 respectively. The pressure is independent of temperature. This is due to the nearly total energy transfer in collisional plasma. As shown in Fig. 7, almost all of the electrical energy is transferred to the flow for $\alpha > 1$. Given flame collision parameters are typically >100, the collisional impact energy term $\epsilon_{w,\alpha>1}$ in Eq. (12) can be neglected. Then energy transfer and thus pressure is dependent on the non-dimensionalized potential, which has a $1/kT_e$ term. The force density for a fixed D is also independent of the temperature. If D is taken as the sheath thickness however, then the force density varies with temperature through the Debye length. Both quantities vary linearly with ion density as the energy transfer is per ion.

Note that these values are obtained for a predetermined distance over which the electric field acts, i.e., setting the sheath thickness to 0.5 cm for a 15 kV potential to obtain a 30 kV/cm field. In reality, the sheath thickness for a given potential is affected by multiple variables as previously shown. If the sheath is determined self-consistently, a 15 kV potential gives a collisional sheath thickness of 1.19 cm, which is a 12.6 kV/cm field. Of course if the distance is physically held at 0.5 cm somehow, then a 30 kV/cm field would be obtained. In this case the sheath (1.19 cm) is larger than the physical spacing (0.5 cm), thus would span the entire distance. The sheath formulation of the ionic wind force does not exactly match the maxima derived by Lawton and Weinberg, but do have reasonable agreement given the different analysis methods.

3.3. Thermal equilibrium and relaxation times

The work presented in this paper makes the assumption of thermal equilibrium between electrons, ions, and neutrals. This allows an easy determination of charged species temperatures, and velocities, and is often used in the literature. The validity of the equilibrium assumption can be examined by considering the relaxation mean free paths of ions and electrons. When two particles collide, energy is transferred from the faster particle to the slower one. When the two particles have equal or similar mass (i.e., ion–neutral collisions), half of the fast particle's energy is transferred as shown by McDaniel [41]. If the fast particle is much lighter than the second particle (i.e., electron–neutral collisions), the fraction of energy transferred is only $2m/M$, where m is the fast particle's mass and M is the mass of the second particle. For electron–N_2, this is 3.91×10^{-5}. This is an exponential decay process.

To transfer 99.9% of an ion or electron's energy to neutrals, an ion requires ~10 collisions while electrons require ~175,000 collisions. The momentum transfer mean free path for ion–N_2 and electron–N_2 are 2.2×10^{-4} and 3.89×10^{-3} mm respectively. Thus ion and electron relaxation and equilibration mean free path are approximately 2.2×10^{-3} mm and 68 cm. This very simple analysis would seem to indicate that ions reach thermal equilibrium almost immediately after creation within the reaction zone, while electron may never reach thermal equilibrium. The latter is a rather surprising result, but it does not necessarily mean electrons are orders of magnitude more energetic than ion or neutrals. Electrons are likely created at temperatures similar to that of neutrals, thus starting near equilibrium, as chemical ionization is not a very energetic process. Electrons may also be lost through recombination reactions. Lastly, due to the mass difference between electrons and neutrals, electrons are not the primary method of momentum transfer for the ionic wind. A more in depth consideration of particle collision in flames may be needed, but that is not the focus of this paper, and may be the subject of future work.

4. Conclusions

In this paper plasma sheath theory is applied to collisional flame plasma in an effort to understand the basic mechanisms. It was analytically shown that the sheath at the positive electrode is less than 1 V, only tens of microns thick, and independent of the applied voltage. The cathode sheath grows with applied voltage and extends to multiple centimeters. The results explain why a positive burner causes little or no change to the flame. The ionic wind force is examined by equating the ion energy loss from collisions to the energy transferred to the flow. The results match well to the original maximum derived by Lawton and Weinberg. The results of this work provide a foundation for future theoretical development of electric field modified flames and helps explain some of the variable flame behaviors reported in the literature.

The equations presented here can be used to approximate the sheath and field properties by the following process:

(1) Knowing or approximating n_e, T_e, and V, calculate η and λ_D.
(2) Calculate the collision parameter from $\alpha = \lambda_D/\lambda_{MFP}$, where $\lambda_{MFP} = 1/n_n\sigma_{in}$.
(3) The anode sheath potential can be found from Eq. (3). The cathode sheath potential can be taken as the applied potential.
(4) The sheath thickness can then be calculated from Eq. (4) and $d = D/\lambda_D$.
(5) The energy, force density, and pressure that result from the electric field can be calculated from Eqs. (12)–(14).
(6) Property variations within the sheath can be roughly calculated from Eqs. (3), (14), and (13) for the potential, electric field, and ion velocity. Higher accuracy can be obtained by numerically solving the governing Eqs. (24) and (25).

The 1D results presented here make simplifying assumptions, such as constant temperature and plasma density that may not hold for an actual flame. Further work is needed to develop a higher fidelity model with spatial property variation to better capture and understand the plasma behavior and its effects on the flame.

Acknowledgments

This work is sponsored by the University of Alabama in Huntsville; the author is very appreciative of the support. The author would like to thank Dr. Logan Williams for fruitful discus-

sions and insight, and Dr. Babak Shotorban for mathematical assistance.

Appendix A. Sheath solution derivation

The conservation equations for the two-fluid model as given by Sheridan and Goree are [39]:

$$n_s = n_o \exp\left(-\frac{eV_s}{kT_e}\right), \tag{15}$$

$$\frac{d}{dx}(n_i v_i) = 0, \tag{16}$$

$$m_i v_i \frac{dv_i}{dx} = -e\frac{dV_s}{dx} - m_i(n_n \sigma_{in} v_i) v_i, \tag{17}$$

$$\frac{d^2V_s}{dx^2} = -\frac{e}{\epsilon_o}(n_i - n_e). \tag{18}$$

Eqs. (15)–(18) can be combined to obtain a pair of coupled differential equations for the sheath.

$$v_i \frac{dv_i}{dx} = -\frac{e}{m_i}\frac{dV_s}{dx} - n_n \sigma_{in} v_i^2, \tag{19}$$

$$\frac{d^2V_s}{dx^2} = \frac{e}{\epsilon_o}\left[\frac{v_o}{v_i} - \exp\left(\frac{eV_s}{kT_e}\right)\right]. \tag{20}$$

The ion density is obtained from the continuity equation $n_i v_i = n_o v_o$. The two governing equations can be non-dimensionalized by scaling the potential, distance, and velocity by the appropriate factors.

$$\eta = -\frac{eV_s}{kT_e}, \tag{21}$$

$$\xi = \frac{x}{\lambda_D}, \tag{22}$$

$$u = \frac{v}{v_B}. \tag{23}$$

The dimensional sheath thickness is $d = D/\lambda_D$. Substituting the dimensionless variables into Eqs. (19) and (20), and using the definition of the collision parameter, α, previously defined, the governing equations become

$$uu' = \eta' - \alpha u^2, \tag{24}$$

$$\eta'' = \frac{u_o}{u} - \exp(-\eta), \tag{25}$$

where the prime denotes derivative with respect to ξ. The boundary conditions for the governing equations are given at the wall ($\xi = d$) and at the sheath edge ($\xi = 0$). At the wall, $\eta(d) = \eta_w$. At the sheath edge, $\eta(0) = 0$, $\eta'(0) = 0$, and $u(0) = u_o$. From here the equations can be solve numerically for $\eta(\xi)$ and u(ξ) using schemes such as Runge–Kutta.

The analytical solutions are obtained by simplifying the governing equations. For a collisional sheath, the convective term in the momentum equation, uu', can be neglected as the ion motion will be collisionally dominated. Additional, as the sheath is a pure ion sheath (electron repelling) the electron density contribution in Poisson's equation can be neglected. Thus the governing Eqs. (24) and (25) become

$$u = \sqrt{\frac{\eta'}{\alpha}}, \tag{26}$$

$$\eta'' = \frac{u_o}{u} = \frac{\alpha^{1/2} u_o}{(\eta')^{1/2}}. \tag{27}$$

Eq. (27) can be integrated by setting $g(\xi) = \eta'$, with the initial condition $g(0) = \eta'(0) = 0$. Thus

$$\int_0^g g^{1/2} dg_1 = \int_0^\xi \alpha^{1/2} u_o d\xi_1, \tag{28}$$

resulting in

$$g = \frac{d\eta}{d\xi} = \left(\frac{3}{2} u_o \alpha^{1/2} \xi\right)^{2/3}, \tag{29}$$

which is an expression for the electric field as a function of position. Eq. (29) can now be integrated again to obtain a function for η,

$$\eta = \frac{3}{5}\left(\frac{3}{2}u_o\right)^{2/3} \alpha^{1/3} \xi^{5/3}. \tag{30}$$

Taking Eq. (30) at the wall ($\xi = d$, $\eta = \eta_w$), we obtain an expression for the collisional sheath thickness.

$$d = \left[\frac{500}{243}\frac{\eta_w^3}{\alpha u_o^2}\right]^{1/5}. \tag{31}$$

For a collisionless sheath, analytical expressions are obtained by setting $\alpha = 0$ in Eq. (27) for collisionless, and letting $u_o \approx 1$ from the Bohm criterion thus making $u_o \ll \eta$, and also neglecting the electron density in Poisson's equation.

$$uu' = \eta'$$
$$\tfrac{1}{2}u^2 = \tfrac{1}{2}u_o^2 + \eta = \eta, \tag{32}$$

$$\eta'' = \frac{u_o}{\sqrt{2\eta}}. \tag{33}$$

Multiple both size by η'

$$\frac{d\eta}{d\xi}\frac{d^2\eta}{d\xi^2} = \frac{u_o}{\sqrt{2}}\eta^{-1/2}\frac{d\eta}{d\xi}. \tag{34}$$

Using the chain rule

$$\frac{d\eta}{d\xi}\frac{d^2\eta}{d\xi^2} = \frac{1}{2}\frac{d}{d\xi}\left(\frac{d\eta}{d\xi}\right)^2, \tag{35}$$

we can integrate to obtain η'

$$\int d\left(\frac{d\eta}{d\xi}\right)^2 = \frac{u_o}{\sqrt{2}}\int \eta^{-1/2} d\eta$$
$$\frac{d\eta}{d\xi} = \left[\frac{1}{2}\frac{u_o}{\sqrt{2}}\eta^{1/2}\right]^{1/2}. \tag{36}$$

Integrating once more gives an expression for η and then d.

$$\eta = \frac{3^{4/3}}{2^{5/3}} u_o^{2/3} \xi^{4/3}, \tag{37}$$

$$d = \frac{2^{5/4}}{3}\frac{\eta_w^{3/4}}{u_o^{1/2}}. \tag{38}$$

Appendix B. Ion energy transfer derivation

Eq. (24) gives the non-dimensionalized form of the momentum equation. For a collisionless plasma ($\alpha = 0$), it can be integrated for the ion velocity as a function of potential [39].

$$\frac{1}{2}u^2 = \frac{1}{2}u_o + \eta. \tag{39}$$

The ion kinetic energy can be non-dimensionalized as $\epsilon = (1/2m_i v_i^2)/kT_e$. At the wall or electrode, ions impact with an energy

$$\epsilon_{w,\alpha} = 0 = \frac{1}{2}u_w^2 = \frac{1}{2}u_o^2 + \eta_w. \tag{40}$$

As this is the impact energy for a collisionless sheath, i.e., no energy loses, this also equals the maximum ion energy for a given sheath potential ϵ_{max}. For a collisional sheath, the convective term uu' in Eq. (24) can be neglected as the particle's motion will be collsionally dominated. Thus

$$u = \sqrt{\frac{\eta'}{\alpha}}, \tag{41}$$

and η' can be obtained from Eq. (25)

$$\eta' = \left(\frac{3}{2}u_o\right)^{2/3}\alpha^{1/3}\xi^{2/3}, \tag{42}$$

and the collisional impact energy is then

$$\epsilon_{w,\alpha>1} = \frac{1}{2}u_w^2 = \frac{1}{2}\frac{\eta'}{\alpha} = \frac{1}{2}\left(\frac{3}{2}u_o\right)^{2/3}\alpha^{-2/3}\xi^{2/3} = \frac{1}{2}\left(\frac{5}{2}\frac{u_o\eta_w}{\alpha^{8/3}}\right)^{2/5}. \tag{43}$$

This is the energy with which ions impact the electrode after moving through a collisional sheath where energy is lost to neutral collisions. The difference between the maximum impact energy from the collisionless case and the collisional case for a given sheath potential and collision parameter gives the total energy lost to the flow per ion.

$$\Delta\epsilon = \frac{1}{2}u_o^2 + \eta_w - \frac{1}{2}\left(\frac{5}{2}\frac{u_o\eta_w}{\alpha^{8/3}}\right)^{2/5}. \tag{44}$$

References

[1] A.P. Chattock, Philos. Mag. Ser. 5 (48) (1899) 401–420.
[2] D. Wisman, S. Marcum, B. Ganguly, Combust. Flame 151 (2007) 639–648.
[3] J. van den boom, A. Konnov, A. Verhasselt, V. Kornilov, L. Degoey, et al., Proc. Combust. Inst. 32 (2009) 1237–1244.
[4] D.W. Blair, F.C. Shen, Combust. Flame 13 (1969) 440–442.
[5] H. Calcote, R. Pease, Ind. Eng. Chem. (1951).
[6] A. Sakhrieh, G. Lins, F. Dinkelacker, T. Hammer, A. Leipertz, et al., Combust. Flame 143 (2005) 313–322.
[7] A. Ata, J.S. Cowart, A. Vranos, B.M. Cetegen, Combust. Sci. Technol. 177 (2005) 1291–1304.
[8] J. Kuhl, G. Jovicic, L. Zigan, A. Leipertz, Proc. Combust. Inst. 34 (2013) 3303–3310.
[9] J. Lawton, F.J. Weinberg, Proc. R. Soc. Lond. A 277 (1964) 468–4697.
[10] M. Saito, T. Arai, M. Arai, Combust. Flame 119 (1999) 356–366.
[11] Z. Yuan, U. Hegde, G. Faeth, Combust. Flame 716 (2001) 712–716.
[12] W. Sun, M. Uddi, S.H. Won, T. Ombrello, C. Carter, et al., Combust. Flame 159 (2012) 221–229.
[13] S. Marcum, B. Ganguly, Combust. Flame 143 (2005) 27–36.
[14] H.C. Jaggers, A. Von Engel, Combust. Flame 16 (1971) 275–285.
[15] Y. Wang, G.J. Nathan, Z.T. Alwahabi, K.D. King, K. Ho, et al., Combust. Flame 157 (2010) 1308–1315.
[16] M. Kono, F.B. Carleton, A.R. Jones, F.J. Weinberg, Combust. Flame 78 (1989) 357–364.
[17] M. Saito, M. Sato, K. Sawada, J. Electrostat. 39 (1997) 305–311.
[18] R.J. Bowser, F. Weinberg, Combust. Flame 18 (1972) 296–300.
[19] J. Hu, B. Rivin, E. Sher, Exp. Therm. Fluid Sci. 21 (2000) 124–133.
[20] J.M. Goodings, J. Guo, J.G. Laframboise, Electrochem. Commun. 4 (2002) 363–369.
[21] J.M. Goodings, J. Guo, A.N. Hayhurst, S.G. Taylor, Int. J. Mass Spectrom. 206 (2001) 137–151.
[22] M. Belhi, P. Domingo, P. Vervisch, Combust. Flame 157 (2010) 2286–2297.
[23] J.M. Goodings, D.K. Bohme, C.-W. Ng, Combust. Flame 36 (1979) 27–43.
[24] J. Prager, U. Riedel, J. Warnatz, Proc. Combust. Inst. 31 (2007) 1129–1137.
[25] S.R. Turns, An Introduction to Combustion, second ed., McGraw-Hill, Boston, 2000. p. 411.
[26] Y. Itikawa, J. Phys. Chem. Ref. Data 35 (2006) 31.
[27] H.F. Calcote, I.R. King, Studies of Ionization in Flames by Measure of Langmuir Probes, vol. 5, 5th Symposium (International) on Combustion, 1955, pp. 423–434.
[28] R.A. Heppner, F.L. Walls, W.T. Armstrong, G.H. Dunn, Phys. Rev. A 13 (1976) 1000–1011.
[29] J. Guo, J.M. Goodings, Chem. Phys. Lett. 329 (2000) 393–398.
[30] A. Neau, A. Al Khalili, S. Rosén, A. Le Padellec, A.M. Derkatch, et al., J. Chem. Phys. 113 (2000) 1762.
[31] S.K. Chulkov, Y. V Novakovskaya, Phys. Scr. 80 (2009) 048119.
[32] A. Faure, J. Tennyson, Mon. Not. Roy. Astron. Soc. 340 (2003) 468–472.
[33] M.T. Leu, M.A. Biondi, R. Johnsen, Phys. Rev. A 7 (1973) 292–298.
[34] F.F. Chen, Introduction to Plasma Physics and Controlled Fusion, vol. 1, second ed., Plasma Physics, Springer, New York, 2006.
[35] D.M. Goebel, I. Katz, Fundamentals of Electric Propulsion: Ion and Hall Thrusters, Jet Propulsion Laboratory, Pasadena, 2008.
[36] M. Mitchner, C.H.J. Kruger, Partially Ionized Gases, John Wiley & Sons Inc., 1973.
[37] K.-U. Riemann, J. Phys. D Appl. Phys. 24 (1991) 493–518.
[38] L. Oksuz, N. Hershkowitz, Plasma Sources Sci. Technol. 14 (2005) 201–208.
[39] T.E. Sheridan, J. Goree, Phys. Fluids B Plasma Phys. 3 (1991) 2796.
[40] J. Schmidt, S. Kostka, S. Roy, J. Gord, B. Ganguly, Combust. Flame 160 (2013) 276–284.
[41] E.W. McDaniel, Collisional Phenomena in Ionized Gases, Wiley, New York, 1964.